ORIGINAL PAPER

Distinct interferon response in bat and other mammalian cell lines infected with *Pteropine orthoreovirus*

Ronald Tarigan[1] · Tetsufumi Katta[1] · Hitoshi Takemae[1] · Hiroshi Shimoda[2] · Ken Maeda[3] · Atsuo Iida[1] ·
Eiichi Hondo[1]

Abstract
Bats serve as natural hosts of *Pteropine orthoreovirus* (PRV), an emerging group of bat-borne, zoonotic viruses. Bats appear to possess unique innate immune system responses that can inhibit viral replication, thus reducing clinical symptoms. We examined the innate immune response against PRV and assessed viral replication in cell lines derived from four bat species (*Miniopterus fuliginosus*, *Pteropus dasymallus*, *Rhinolophus ferrumequinum*, and *Rousettus leschenaultii*), one rodent (*Mesocricetous auratus*), and human (*Homo sapiens*). The expression levels of pattern recognition receptors (PRRs) (*TLR3*, *RIG-I*, and *MDA5*) and interferons (*IFNB1* and *IFNL1*) were higher and PRV replication was lower in cell lines derived from *M. fuliginosus*, *R. ferrumequinum*, and *R. leschenaultii*. Reduction of *IFNB1* expression by the knockdown of PRRs in the cell line derived from *R. ferrumequinum* was associated with increased PRV replication. The knockdown of *RIG-I* led to the most significant reduction in viral replication for all cell lines. These results suggest that *RIG-I* production is important for antiviral response against PRV in *R. ferrumequinum*.

Abbreviations

CPE	Cytopathic Effect
DMEM	Dulbecco's Modified Eagle Medium
dpi	Days Post-Infection
dsRNA	Double-Stranded RNA
FBS	Fetal Bovine Serum
IFNB1	Interferon-Beta
IFNL1	Interferon-Lambda-1
MERS-CoV	Middle East Respiratory Syndrome Coronaviruses
MDA5	Melanoma Differentiation-Associated Protein 5
MOI	Multiplicity of Infection
NBV	Nelson Bay Orthoreovirus
NLRP3	NLR Family Pyrin Domain Containing 3
PRRs	Pattern Recognition Receptors
PRVs	*Pteropine orthoreoviruses*
PRV50G	*Pteropine orthoreovirus* Strain Garut-50
RIG-I	Retinoic Acid-Inducible Gene I
SARS-CoV	Severe Acute Respiratory Syndrome Coronaviruses
TLRs	Toll-Like Receptors
TNF-α	Tumor Necrosis Factor Alpha

Introduction

Bats are well recognized as natural hosts of multiple highly pathogenic zoonotic viruses, such as Marburg virus [1], SARS-CoV [2], MERS-CoV [3], Hendra virus [4], Nipah virus [5], and Ebola virus [6]. Viral transmission to humans directly from bats or via other animals as intermediate hosts has occurred previously, causing fatal outbreaks in humans

and suggesting an important role of bats in disease transmission [1, 7–9].

Pteropine orthoreoviruses (PRVs) are bat-borne viruses (family *Reoviridae*, genus *Orthoreovirus*). The genomes of these viruses contain ten double-stranded RNA (dsRNA) segments. The first PRV to be isolated, Nelson Bay orthoreovirus (NBV; previously known as Nelson Bay virus), was isolated from the gray-headed flying fox (*Pteropus poliocephalus*) in Australia in 1968 [10]. Since then, PRVs have been isolated from some frugivorous and nectarivorous bats in Malaysia, Indonesia, Philippines, and China [11–14]. Viral transmission from bats to humans occurs in these regions, as revealed by viral isolation from people living near bat roosts in Malaysia and by serological studies conducted in Malaysia, Vietnam, and Singapore [15–18]. Non-fatal imported cases of PRV have been reported in Japan and Hong Kong in patients presenting with an acute respiratory syndrome, who had previously traveled to Bali and Indonesia [19, 20]. Notably, the virulence of PRV may be altered by the process of reassortment, much like the influenza virus [21].

It is speculated that bats, as the natural hosts of PRVs, do not show the same clinical symptoms as those observed in humans and mice [22, 23]. The limited clinical symptoms observed in bats after experimental infection with highly pathogenic viruses such as Nipah virus, Ebola virus, and MERS-CoV suggest an innate immune response peculiar to bats [24–26]. The innate immune response against dsRNA viruses is initiated upon sensing by pattern recognition receptors (PRRs), which stimulate the production of interferons (IFNs) and cytokines [27]. The PRRs for dsRNA are toll-like receptors-3 (TLR3), retinoic acid-inducible gene-I (RIG-I), and melanoma differentiation-associated protein 5 (MDA5); these are highly expressed in bat cell lines and promote greater IFN stimulation as part of the bat antiviral response than that observed in other mammalian cell lines [28–30]. We hypothesize that an increased IFN response is responsible for suppressing PRV in bat cell lines. Here, we examine the IFN response in cell lines derived from four bat species (*Miniopterus fuliginosus*, *Pteropus dasymallus*, *Rhinolophus ferrumequinum*, and *Rousettus leschenaultii*), from human (*Homo sapiens*), and from Syrian hamster (*Mesocricetous auratus*). The bat cell lines used in this study have been utilized for analysis of Ebola and Marburg virus [31], encephalomyocarditis and Japanese encephalitis viruses [30], Lloviu virus [32, 33], bat-derived influenza virus [34], and African bat mumps virus [35].

Materials and methods

Cell lines and viruses

The cell lines BHK-21 (Syrian hamster, kidney), HEK293T (human, kidney), FBKT1 (Ryukyu flying fox, *P. dasymallus*, kidney), DEMKT1 (Leschenault's rousette, *Rousettus leschenaultii*, kidney), BKT1 (Greater horseshoe bat, *R. ferrumequinum*, kidney), YUBFKT1 (Eastern bent-wing bats, *M. fuliginosus*, kidney), and Vero JCRB9013 (African green monkey, *Cercopithecus aethiops*, kidney) were maintained in Dulbecco's Modified Eagle's Medium (DMEM; Nissui, Tokyo, Japan) supplemented with 10% fetal bovine serum (FBS; HyClone, Logan, USA), 2% L-Glutamine (Sigma, Milwaukee, Wisconsin, USA), 0.14% sodium hydrogen carbonate (NaHCO$_3$; Sigma, Milwaukee, USA), and penicillin–streptomycin (Meiji, Tokyo, Japan) at a final concentration of 100 U/mL and 0.1 μg/mL. The bat kidney cell lines were established as previously described [32, 36]. The PRV used in this study, strain Garut-50 (PRV50G), was isolated from a rectal swab of a greater flying fox (*Pteropus vampyrus*) from Garut Regency, West Java Province, Indonesia. PRV50G was propagated in Vero JCRB9013 cells, and the viral titer was measured by plaque assay.

Detection of virus RNA and host-factor mRNA in the cells

The cells were seeded at a concentration of 5×10^5 cells/well in a 6-well plate to obtain 50–80% confluency in most of the cells in 24 h. Cells were infected with PRV50G at a multiplicity of infection (MOI) of 0.1 in a Biosafety Level 2 laboratory. The RNA copy number of inoculating virus is 1.78×10^4 viral RNA copy number/well. The viruses were allowed to adsorb onto the cells for 2 h in DMEM medium containing 2% FBS. The inoculum was removed and the cells were rinsed twice with DMEM medium containing 2% FBS to remove the residual inoculum. Then, fresh DMEM medium containing 2% FBS was added to the cells. This virus infection method was used in all assays.

RNA extraction was performed using ISOGEN II (Nippon Gene, Japan), and RNA clean-up was performed using RNeasy Mini Kit (QIAGEN, Hilden, Germany). First-strand cDNA synthesis was performed using ReverTra Ace (Toyobo, Osaka, Japan).

The expression levels of *TLR3*, *RIG-I*, *MDA5*, *IFNB1*, *IFNL1*, *TNF-α*, and glyceraldehyde-3-phosphate dehydrogenase (*GAPDH*, housekeeping gene) in mock- and PRV50G-infected cells were determined by qRT-PCR. The primer sequences are listed in Supplementary Table 1. The Roche LightCycler 96 system (Roche, Mannheim, Germany) was used in conjunction with Thunderbird SYBR qPCR Mix (Toyobo, Osaka, Japan) per the manufacturer's instructions. For qRT-PCR, after the pre-denaturation step (95 °C, 60 s), three-step cycling was performed at 95 °C/60 s, 55 °C/30 s, and 72 °C/30 s for 40 cycles. Melting curve analysis was performed at 95 °C/10 s, 60 °C/60 s, and 97 °C/1 s to generate the dissociation curve. Relative expression level is expressed as reciprocal of ΔCt (the PCR cycle at which the

product is measurable and normalized to Ct for *GAPDH*) [37]. The relative fold change in gene expression between two groups of cells (infected/mock) was calculated after normalizing the Ct values using the value for *GAPDH*.

For comparative quantitative analysis of viral genome copies, absolute quantification was performed with specific primers for the S4 segment (5′- TTGGATCGAATG GTGCTGCT, 5′- TCGGGAGCAACACCTTTCTC) with target nucleotides (256–415) of the S4 genome segment of PRV50G (GenBank accession number LC494117.1) and has expected size of PCR amplicon 159 bp. PCR-amplified fragments were serially diluted and used for the creation of standard curves. The exact number of copies was calculated using the standard curve.

Cell viability assay

Cells were seeded at a concentration of 5×10^4 cells/well in a 24-well plate and were infected with PRV50G at MOI of 0.1. Both mock- and PRV50G-infected cells were washed with PBS and were harvested using 0.25% Trypsin–EDTA (Gibco, Ontario, Canada) at 1, 2, 3, 4, 5, 6, and 7 days post-infection (dpi). Assessment of cell growth (cell viability and total live cell numbers) was carried out by trypan blue dye exclusion test. Cell suspensions were mixed with an equal volume of 0.4% trypan blue solution (Chroma-Gesellschaft Schmid, Stuttgart, Germany). Unstained or live cells were counted using the automated Cell Counter model R1 (Olympus, Tokyo, Japan). Relative viabilities of PRV50G-infected cells are shown as the ratio between the live cell numbers of PRV50G-infected cells and mock-infected cells on the same days. Relative viabilities of viral-infected cells are shown as % of mock-infected cells.

Knockdown of pattern recognition receptors and *TNF-α*

Phosphorothioate antisense RNA oligonucleotide (s-oligo) against *TLR3* (5′-GCACAAUUCUGGCUCCAGUTT-3′), *RIG-I* (5′-AUCUGAGAAGGCAUUCAACTT-3′), and *MDA5* (5′-UGACACUUCCUUCUGCCAATT-3′) of three bat species (*R. ferrumequinum*, *R. leschenaultii*, and *M. fuliginosus*), human *TNF-α* (5′-GGCGUGGAGCUGAGA GAUA-3′), and negative control s-oligo (5′-GGUUCGUAC GUACACUGUUCATT-3′) designated from the sequence of *Arabidopsis thaliana* were synthesized by FASMAC Co., Ltd. (Kanagawa, Japan). Three bat cell lines (BKT1, DEMKT1, and YUBFKT1) and HEK293T were transfected with the antisense RNA oligonucleotides (120 pmol) using polyethylenimine [38].

After verification of remarkably decreased expression level of PRRs and *TNF-α* in each cell line by qRT-PCR 2 days after gene knockdown, the knockdown cells were

infected with PRV50G at an MOI of 0.1. RNA extraction and first-strand cDNA synthesis using 500 ng of total RNA, quantified by nanodrop, were performed at 1 dpi. The expression levels of *TLR3*, *RIG-I*, *MDA5*, *IFNB1*, *IFNL1*, *TNF-α*, and *GAPDH* and viral copy numbers in both mock- and PRV50G-infected cells were determined by qRT-PCR.

Statistical analysis

All statistical analyses were performed using Prism software (version 9.0, GraphPad Software Inc.). Significant statistical differences were calculated by two-tailed Mann–Whitney *U* test or one-way ANOVA followed by Dunnett's test. $P < 0.05$ was considered statistically significant.

Results

Cytopathic effect of PRV50G in cell lines

As PRVs are fusogenic orthoreoviruses [39], the cytopathic effect (CPE) after PRV infection is characterized by syncytia formation. The syncytial CPE was observed in non-bat cell lines (BHK-21 and HEK293T) at 1 dpi (Fig. 1a). One bat cell line (FBKT1) showed a syncytial CPE at 2 dpi. Cell viability in those lines rapidly decreased at 1–2 dpi, and complete cell lysis was observed at 3 dpi (Fig. 1b). In contrast, the other bat cell lines (BKT1, DEMKT1, and YUB-FKT1) did not show a syncytial CPE, although a subtotal destruction CPE was observed at 3 dpi for BKT1 and at 4 dpi for DEMKT1 and YUBFKT1 (Fig. 1a). Cell viability in those cell lines decreased slowly (Fig. 1b), and complete cell lysis was observed at 7 dpi. Until 7 days, a decrease in cell viabilities of mock-infected cells was observed as a result of overgrowth (Supplementary Fig. 1).

Viral replication and expression of PRRs and IFNs

Viral replication was observed in all cell lines at 1 dpi (Fig. 2a). The cell lines BHK-21, HEK293T, and FBKT1 showed significantly higher viral genome titers than the bat cell lines BKT1, DEMKT1, and YUBFKT1. The viral genome titers in BKT1, DEMKT1, and YUBFKT1 were still low until 4 dpi when the CPE in all cell lines was observed (Fig. 2b). Two PRRs (*RIG-I* and *MDA5*) were up-regulated in two bat cell lines (BKT1 and YUBFKT1), and one PRR (*RIG-I*) was up-regulated in DEMKT1 (Fig. 2d and e). In contrast, *TLR3* was only up-regulated in YUBFKT1 (Fig. 2c). Both BHK-21 and FBKT1 displayed high viral replication levels; all PRRs were down-regulated in BHK-21, while no changes in expression level were observed in FBKT1. Conversely, *TLR3* and *MDA5* were up-regulated in HEK293T (0.060 ± 0.001 versus 0.087 ± 0.003, $p = 0.002$

Fig. 1 Cytopathology and cell viabilities in bats and non-bat cell lines after PRV50G infection. **a** Cytopathic effect (CPE) at different days post-infection (dpi) in bats and non-bat cell lines infected with PRV50G at a multiplicity of infection (MOI) of 0.1. Syncytial CPE is indicated by an arrow. **b** The relative viabilities of the six cell lines following PRV50G infection at a multiplicity of infection (MOI) of 0.1 until 7 dpi. Relative viabilities = number of live cells in viral-infected cells/number of live cells in mock-infected cells. The relative viabilities of each virus-infected cell are shown as % of mock-infected cells. Data are shown as the mean of $n = 3$ independent biological replicates ± SD
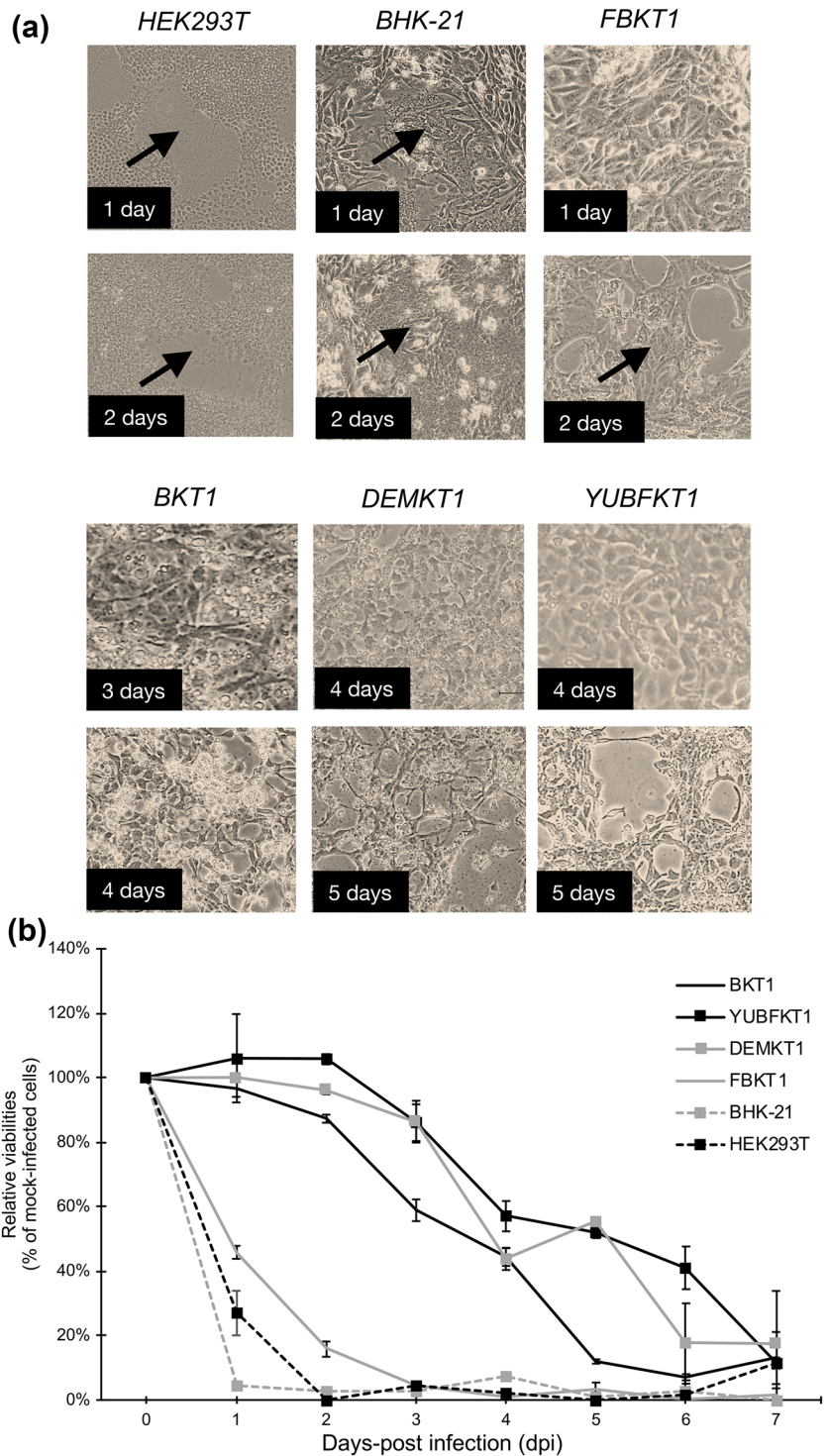
for *TLR3* and 0.057 ± 0.002 versus 0.066 ± 0.001, $p = 0.001$ for *MDA5*, Table 1); however, the expression levels of TLR3 and MDA5 in HEK293T were lower than all bat cell lines, except for BKT1 (Fig. 2c, e). *IFNB1* was highly up-regulated in BKT1 and YUBFKT1, and to a lesser extent in HEK293T. Surprisingly, *IFNB1* was not up-regulated in DEMKT1, although that cell line showed lower PRV

replication (Fig. 2f). *IFNL1* was up-regulated in YUBFKT1, which showed low viral replication, and was up-regulated to a lesser extent in cell lines FBKT1 and HEK293T, which both showed high viral replication (Fig. 2g). The expression levels of *IFNB1* and *IFNL1* could not be measured in

Fig. 2 PRV50G replication and relative expression of pattern recognition receptors and interferons in bats and non-bat cell lines after PRV50G infection. **a** The total PRV50G genome RNA in six cell lines after infection at a MOI of 0.1 at 1 dpi. Total virus genome RNA are expressed as Log_{10} virus genome copies/well ($n=3$, mean $\pm$ SD). Statistical significance was calculated using one-way ANOVA, followed by Dunnett's test. *$p<0.05$, **$p<0.01$, ***$p<0.001$, *ns* not significant vs HEK293T group. **b** The total PRV50G genome RNA in BKT1, DEMKT1, and YUBFKT1 infected with PRV50G at a multiplicity of infection (MOI) of 0.1 until 4 dpi. Total virus genome RNA are expressed as Log_{10} virus genome copies/well ($n=3$, mean $\pm$ SD). **c** Relative mRNA expression levels of *TLR3*, **d** *RIG-I*, **e** *MDA5*, **f** *IFNB1*, and **g** *IFNL1* in six cell lines after PRV50G infection at an MOI of 0.1 at 1 dpi. Expression levels of *IFNB1* in BHK-21 cells and *IFNL1* in BKT1 and DEMKT1 cells could not be measured. Relative expression level is expressed as reciprocal of ΔCt (the PCR cycle at which the product is measurable and normalized to Ct for GAPDH) ($n=3$, mean $\pm$ SD). Statistical significance was determined by the Mann–Whitney test. *$p<0.05$, **$p<0.01$, ***$p<0.001$, *ns* not significant vs mock-infected cells
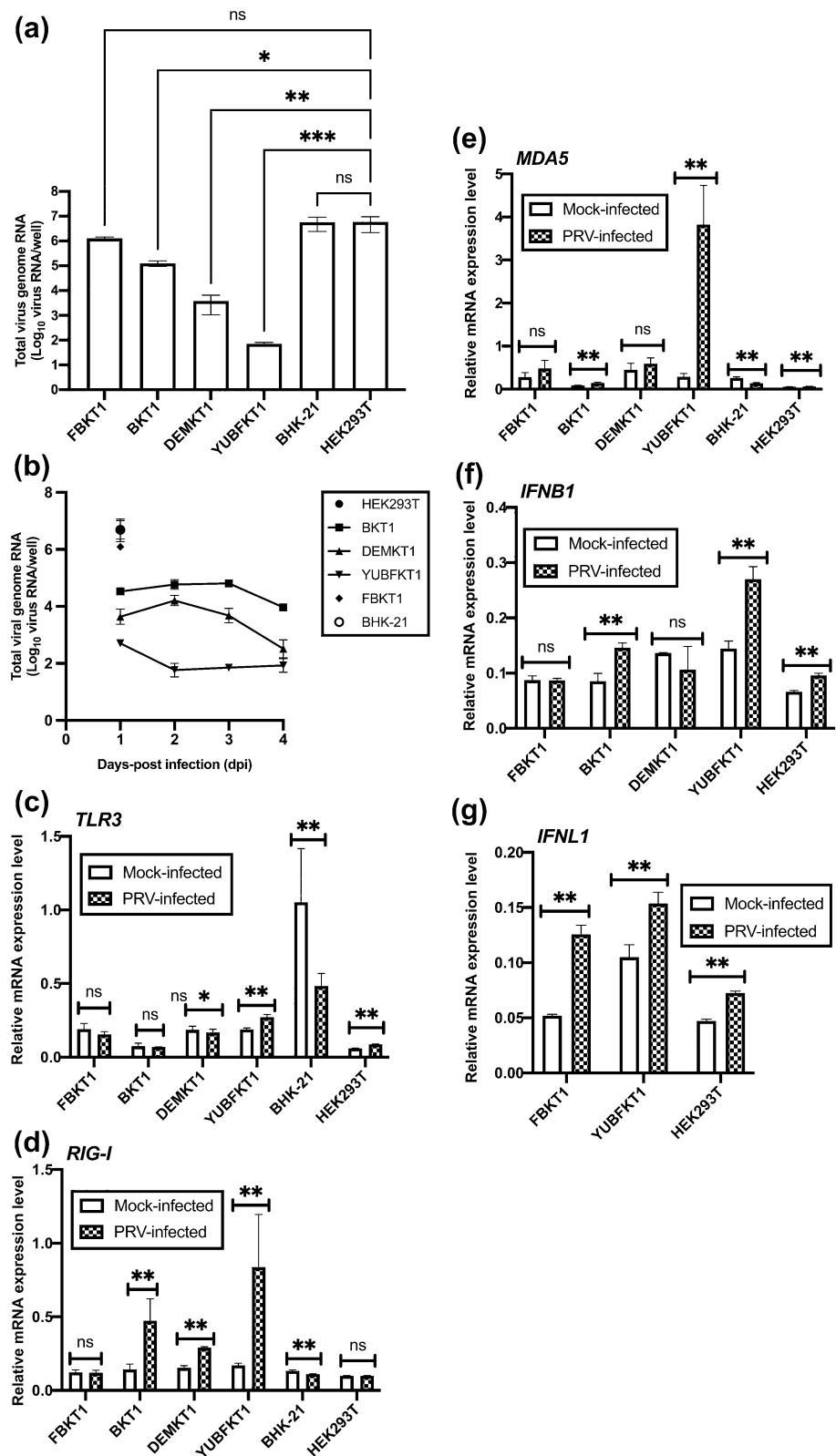
BHK-21, as this cell line is known to be deficient in Type I IFN production, and *IFNL1* is a pseudogene in rodents [40, 41]. The expression of *IFNL1* also could not be measured in two bat cell lines (BKT1 and DEMKT1).

Table 1 Innate immune response against PRV50G and viral replication among six cell lines

Cell lines	Pattern recognition receptors			Interferons		Viral replication
	TLR3	RIG-I	MDA5	B1	L1	
FBKT1[a]	−	−	−	−	↑	High
BKT1[b]	−	↑	↑	↑		Low
DEMKT1[c]	−	↑	−	−		Low
YUBFKT1[d]	↑	↑	↑	↑	↑	Low
HEK293T[e]	↑	−	↑	↑	↑	High
BHK-21[f]	↓	↓	↓			High

[a]*Pteropus dasymallus* (Ryukyu flying fox), [b]*Rhinolophus ferrumequinum* (Greater horseshoe bats), [c]*Rousettus leschenaultii* (Leschenault's rousette), [d]*Miniopterus fuliginosus* (Eastern bent-wing bats), [e]*Homo sapiens* (human), [f]*Mesocricetus auratus* (Syrian hamster)

↑: Up-regulation, −: No change, ↓: Down-regulation

Knockdown of *TNF-α* in HEK293T

The expression of *TNF-α*, a pro-inflammatory cytokine, was up-regulated in FBKT1 and highly up-regulated in HEK293T (Fig. 3a). In contrast, *TNF-α* was down-regulated in BHK-21, while the other bat cell lines did not show a significant change in expression level.

TNF-α that was highly up-regulated in HEK293T with high replication of PRV50G (Figs. 2a and 3a) might positively impact PRV50G replication. An antisense RNA oligonucleotide was used in the knockdown of *TNF-α* in HEK293T, which was performed to determine its role in supporting PRV50G replication. The knockdown of *TNF-α* was confirmed by a reduced expression of it (Supplementary Fig. 2). *TNF-α* might not have any effect on PRV50G replication. The knockdown of *TNF-α* did not change the viral genomic titer significantly (Fig. 3b). PRV50G infection of *TNF-α* knockdown cells resulted in a syncytial CPE (Fig. 3d). Cell viability did not differ between normal and knockdown cells at 12 h post-infection (Fig. 3c).

Knockdown of PRRs in BKT1

Knockdown of *TLR3*, *RIG-I*, and *MDA5* was performed in BKT1, DEMKT1, and YUBFKT1 which showed up-regulation of PRR genes and *IFNB1* without formation of syncytial CPE after PRV50G infection. The knockdown of PRRs was confirmed by the remarkably reduced expression of *TLR3*, *RIG-I*, and *MDA5* in BKT1 (Supplementary Fig. 3). The knockdown of PRRs also depressed the expression of *IFNB1* (Fig. 4a) in BKT1. However, an attempt to knockdown the PRR genes in DEMKT1 and YUBFKT1 failed to suppress the expression of those genes.

After viral infection, the *IFNB1* expression in all types of knockdown cells was still significantly lower than that of the control cells (Fig. 4b). The lowest *IFNB1* expression levels were observed in *RIG-I* knockdown cells. All cells knocked down for PRR genes demonstrated higher viral genome titers than control cells; however, only *RIG-I* knockdown cells exhibited significantly higher PRV50G titers than control cells (Fig. 4c). The syncytial CPE and a rapid decrease in cell viability were observed at 1 dpi in *RIG-I* knockdown cells and at 2 dpi in *MDA5* knockdown cells (Fig. 5a, b, and Supplementary Fig. 4). No syncytial CPE was observed in control cells, and the viability of these cells was higher than that of those knocked down for PRRs.

Discussion

Although all cell lines examined in this study were susceptible to PRV50G, the virulence differed among cell lines. All bat cell lines, except for FBKT1, were more resistant than the other mammalian cell lines, as indicated by a lack of observable syncytial CPE, a slighter decrease of cell viability, and a limited viral replication. The less susceptibility of PRV in Yinpterochiropteran (or Pteropodiformes) bat cell lines (BKT1 and DEMKT1) was different from the kidney cell line derived from the black flying fox (*Pteropus alecto*) that is susceptible to the extensive syncytial formation and high viral replication when exposed to NBV [42]. Low replication of PRV has been reported recently in a bat cell line derived from Yangochiropteran (or Vespertilioniformes) bats, David's myotis (*Myotis davidii*) [43].

The resistance against PRV in most bat cell lines suggests that the innate immune response of some bat species is capable of inhibiting PRV replication (Table 1). The innate immune response is initiated upon viral recognition by PRR proteins, which stimulates the production of IFNs as part of the antiviral response. *TLR3*, *RIG-I*, and *MDA5*, which are responsible for dsRNA virus recognition, are highly expressed in bat cells and enable heightened stimulation of IFN expression. Stimulation by dsRNA molecule induced expression of *TLR3*, *RIG-I*, *MDA5*, and *IFNB1* in bat cells and bat cell lines [28, 29]. The highly up-regulation of *RIG-I* and *MDA5* in YUBFKT1 and *RIG-I* in BKT1 possibly

Fig. 3 Relative expression of *TNF-α* in bats and non-bat cell lines after PRV50G infection and knockdown of *TNF-α* in HEK293T. **a** The relative expression of *TNF-α* in six cell lines after PRV50G infection at a MOI of 0.1 at 1 dpi ($n=3$, mean±SD). Relative expression is expressed as fold of mock-infected, normalized to GAPDH values. Statistical significance was determined by the Mann–Whitney test. *$p<0.05$, **$p<0.01$, ***$p<0.001$, *ns* not significant vs mock-infected cells. **b** The total PRV50G genome RNA, **c** live cell numbers, and **d** syncytial CPE in *TNF-α* knockdown HEK293T cells compared with HEK293T cells transfected with control s-oligo after PRV50G infection at a MOI of 0.1 at 12 h post-infection. Total virus genome RNA are expressed as Log10 virus genome copies/well ($n=3$, mean±SD). Live cell numbers are expressed as×10⁵ cells/mm³. Statistical significance was determined by the Mann–Whitney test. *$p<0.05$, **$p<0.01$, ***$p<0.001$ vs control s-oligo
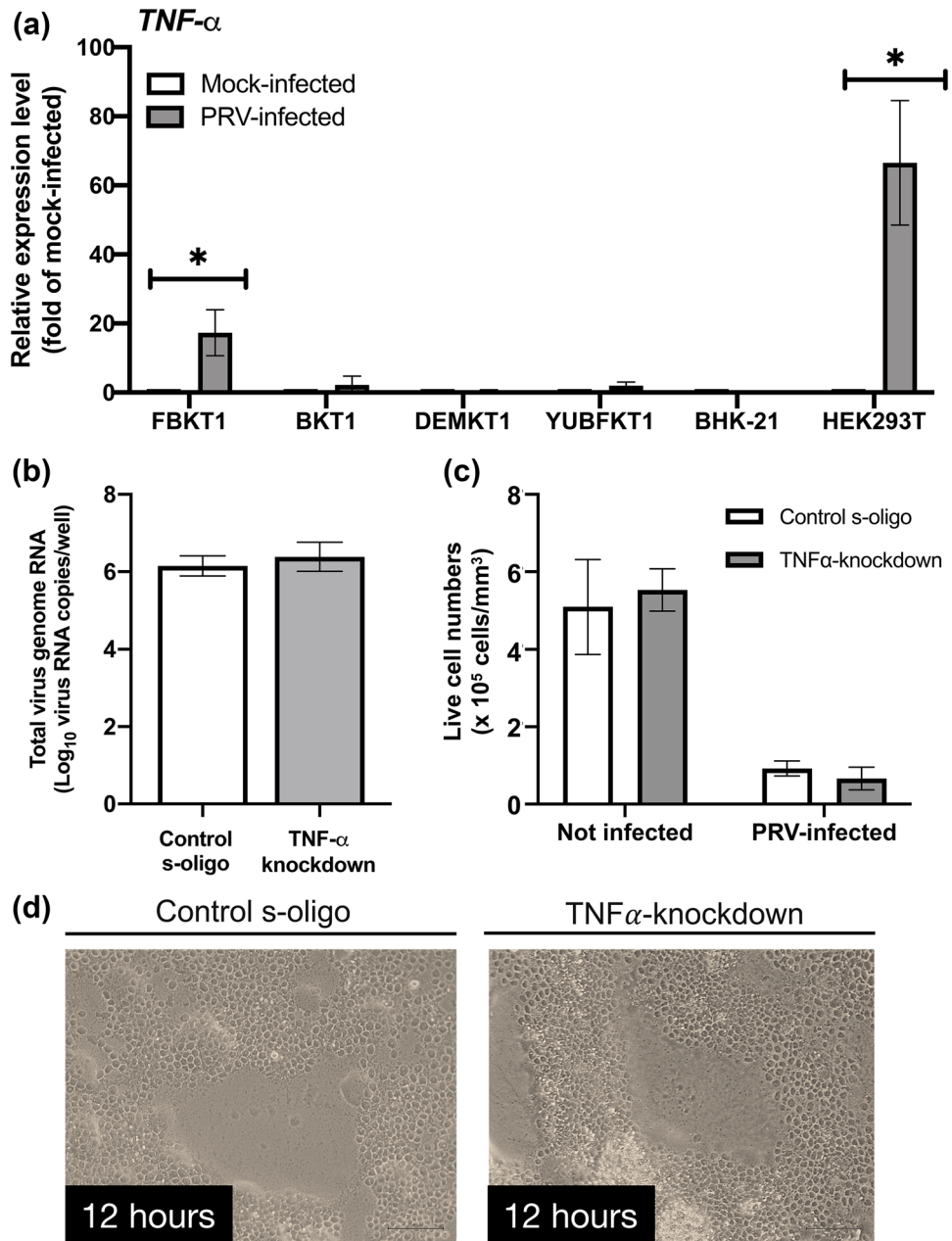
promotes the up-regulation of IFNs and therefore limits PRV replication. Although some PRRs and IFNs were up-regulated in FBKT1 and HEK293T, PRV replication was not significantly reduced in those cell lines. This finding may be related to the fact that the baselines of PRR and IFN expression levels were lower than those in BKT1 and YUB-FKT1. It has been shown that reoviruses can successfully replicate in non-bat cells by inhibiting the activation of proteins involved in the IFN-stimulated antiviral response, such as IFN-induced double-stranded RNA-dependent protein kinase (PKR) and 2′,5′-oligoadenylate synthetase [44, 45]. However, the only different PRRs between bat and non-bat cell lines after PRV infection is *RIG-I*. High expression of

RIG-I is correlated with low viral replication titer in YUB-FKT1. In contrast, low expression of *RIG-I* is correlated with high viral replication titer in HEK293T.

The relatively slight increase in *TNF-α* expression in the bat cell lines might account for the limited inflammation observed after PRV50G infection. A similar slight increase in *TNF-α* expression has been reported in a bat cell line derived from the big brown bat (*Eptesicus fuscus*) after MERS-CoV infection [46]. The c-Rel protein, an NF-κβ-family member, binds the promoter region of the *TNF-α* gene, thus restricting the production of TNF-α [47]. The lack of strong inflammation after PRV (Melaka virus, PRV3M) infection was also reported in immune
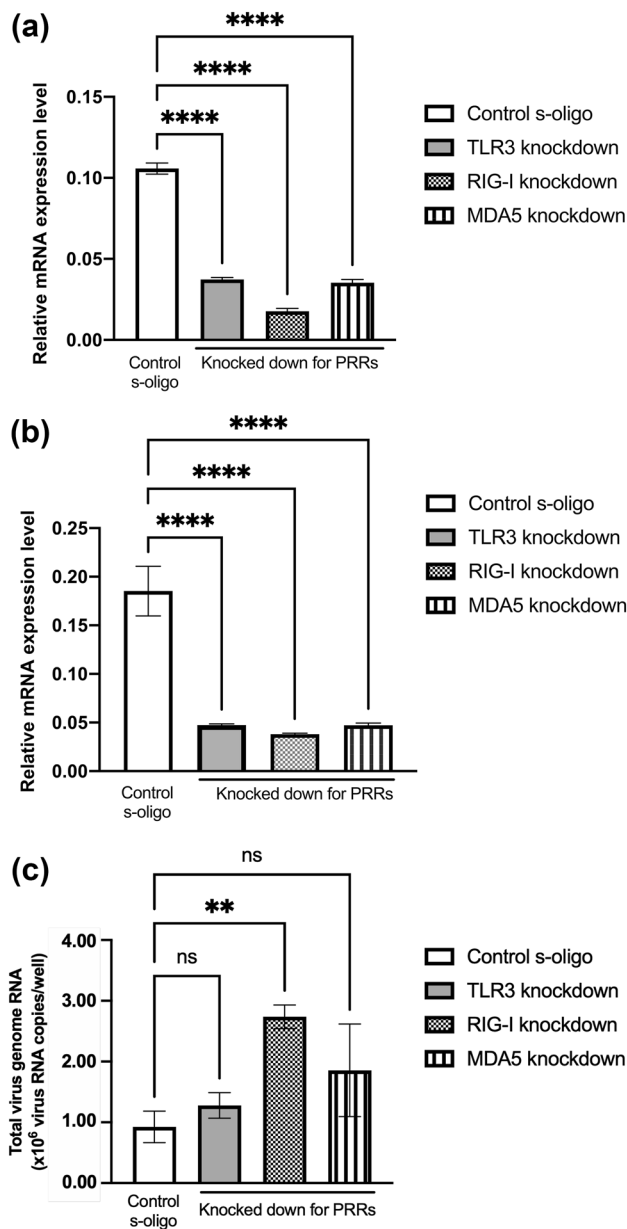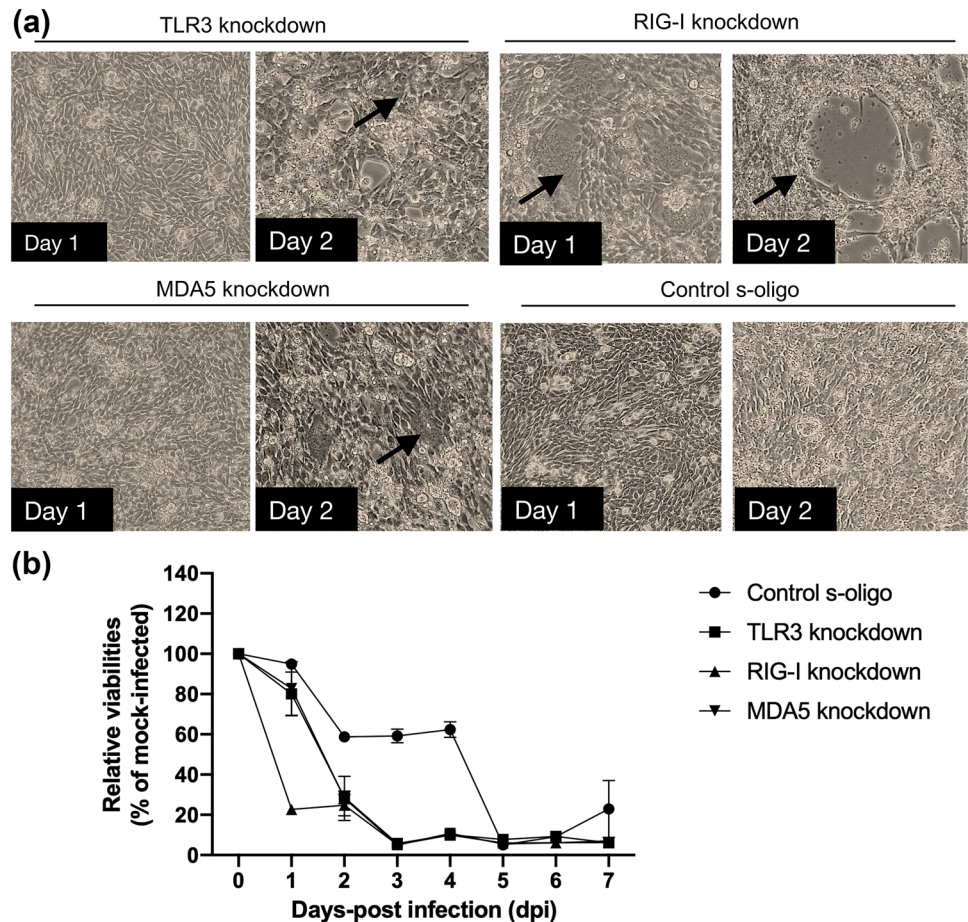
Fig. 4 Knockdown of *TLR3*, *RIG-I*, and *MDA5* in BKT1 cells. **a** The Relative mRNA expression level of *IFNB1* after knockdown of *TLR3*, *RIG-I*, and *MDA5*. **b** Relative mRNA expression of *IFNB1* in BKT1 cells knocked down for *TLR3*, *RIG-I*, and *MDA5* after PRV50G infection at a MOI of 0.1 at 1 dpi. Relative expression level is expressed as reciprocal of ΔCt (the PCR cycle at which the product is measurable and normalized to Ct for *GAPDH*) ($n = 3$, mean ± SD). Statistical significance was calculated using one-way ANOVA, followed by Dunnett's test. $*p < 0.05$, $**p < 0.01$, $***p < 0.001$, *ns* not significant vs control s-oligo group. **c** The total PRV50G genome RNA in BKT1 cells knocked down for *TLR3*, *RIG-I*, and *MDA5* and BKT1 cells transfected with control s-oligo after PRV50G infection at an MOI of 0.1 at 1 dpi. Total virus genome RNA are expressed as $\times 10^6$ virus genome copies/well ($n = 3$, mean ± SD). Statistical significance was calculated using one-way ANOVA, followed by Dunnett's test. *ns* not significant, $*p < 0.05$, $**p < 0.01$, $***p < 0.001$, $****p < 0.0001$, *ns* not significant vs control s-oligo group

cells derived from *P. alecto*; this result was attributed to reduced NLRP3 inflammasome activation, which restricted IL-1β secretion [48]. Such examples of inflammatory response regulation might be crucial in limiting tissue damage and preventing the manifestation of clinical symptoms during viral infection. In contrast, the high up-regulation of *TNF-α* observed in HEK293T suggests a strong inflammatory response might occur in this line, similar to results observed after orthoreovirus infection in murine and human monocyte cell lines [49–51]. However, high TNF-α production apparently has a minimal effect on PRV replication. In addition, the level of other pro-inflammatory cytokines, such as IL-1β, has not been shown to correlate with the replication of Melaka virus (PRV3M) [48].

Knockdown of *TLR3*, *RIG-I*, and *MDA5* resulted in a decreased expression level of *IFNB1*, suggesting that these PRRs are important for stimulating *IFNB1* expression in rhinolophoid (horseshoe) bats. However, *RIG-I* played a more significant role in stimulating an antiviral response against PRV50G than *TLR3* or *MDA5*, as demonstrated by the high rate of viral replication that accompanied a low expression of *IFNB1*. High basal expression of PRRs enables greater viral RNA detection and therefore higher stimulation levels of IFN-stimulated genes (ISGs) and IFNs, such as 2′,5′-oligoadenylate synthetase and RNase L, which can cleave and therefore shorten viral RNA fragments [52]. These shorter viral RNA fragments are recognized by *RIG-I*, which in turn promotes the production of IFNs [53]. The importance of RIG-I-signaling and IFNs in the antiviral response against PRV has also been elucidated in an NBV-resistant mouse fibroblast cell line (L929), and against other RNA viruses, Marburg and Ebola virus in cell lines derived from Rousettus bats. The suppression of *RIG-I* signaling and caspase/cell-death pathways was observed in *P. alecto* kidney cell line (PaKiT03) during NBV infection [54–56]. RIG-I signaling might be the main mechanism for bats to avoid diseases after infection with PRV50G and other RNA viruses. Pre-treatment with IFNs can reduce viral replication and increase the expression of *RIG-I* and ISGs in cell lines that are susceptible to NBV [55, 57, 58]. In addition, several IFN-regulatory factors (IRF1, IRF3, and IRF7) control the IFN-regulated genes (IRGs) response during PRV3M infection [43]. The serine residues that were positively selected in IRF3 from multiple bats also contribute to a higher basal level of IFNs and enhance protection against MERS-CoV in bat cells [46, 59].

In conclusion, *RIG-I* production plays an important role in the antiviral response against PRV50G infection, especially in rhinolophoid (horseshoe) bats. In addition to displaying a robust antiviral response, bats apparently are also capable of suppressing excessive viral-mediated inflammatory responses.

Fig. 5 Cytopathology and cell viabilities in BKT1 cells knocked down for *TLR3*, *RIG-I*, and *MDA5* after PRV50G infection. **a** Cytopathic effect (CPE) at different days post-infection (dpi) in BKT1 cells knocked down for *TLR3*, *RIG-I*, and *MDA5* and BKT1 cells transfected with control s-oligo after infected with PRV50G at a multiplicity of infection (MOI) of 0.1. Syncytial CPE is indicated by arrows. **b** The relative viabilities of BKT1 cells knocked down for *TLR3*, *RIG-I*, and *MDA5* and BKT1 cells transfected with control s-oligo following infection with PRV at MOI of 0.1 until 7 dpi. Relative viabilities = number of live cells in viral-infected cells/number of live cells in mock-infected cells. The relative viabilities of each virus-infected cell are shown as % of mock-infected cells. Data are shown as the mean of $n = 3$ independent biological replicates ± SD

Declarations

Conflict of interest The authors declare that they have no conflicts of interest.

Ethical approval This article does not contain any studies with human participants or animals performed by any of the authors.

References

1. Towner JS, Amman BR, Sealy TK, Carroll SAR, Comer JA, Kemp A, Swanepoel R, Paddock CD, Balinandi S, Khristova ML, Formenty PBH, Albarino CG, Miller DM, Reed ZD, Kayiwa JT, Mills JN, Cannon DL, Greer PW, Byaruhanga E, Farnon EC, Atimnedi P, Okware S, Katongole-Mbidde E, Downing R, Tappero JW, Zaki SR, Ksiazek TG, Nichol ST, Pierre PE (2009) Isolation of genetically diverse Marburg viruses from Egyptian fruit bats. PLoS Pathog 5(7):e1000536. https://doi.org/10.1371/journal.ppat.1000536

2. Li W, Shi Z, Yu M, Ren W, Smith C, Epstein JH, Wang H, Crameri G, Hu Z, Zhang H, Zhanh J, McEachern FH, Daszak P, Eaton BT, Zhang S, Wang LF (2005) Bats are natural reservoirs of SARS-like coronaviruses. Science 310(5748):676–679. https://doi.org/10.1126/science.1118391

3. Memish ZA, Mishra N, Olival KJ, Fagbo SF, Kapoor V, Epstein JH, Al Hakeem R, Durosinloun A, Al Asmari M, Islam A, Kapoor A, Briese T, Daszak P, Rabeeah AA, Lipkin WI (2013) Middle East respiratory syndrome coronavirus in bats, Saudi Arabia. Emerg Infect Dis 19(11):1819–1823. https://doi.org/10.3201/eid1911.131172

4. Halpin K, Young PL, Field HE, Mackenzie JS (2000) Isolation of Hendra virus from pteropid bats: a natural reservoir of Hendra virus. J Gen Virol 81(Pt 8):1927–1932. https://doi.org/10.1099/0022-1317-81-8-1927

5. Chua KB, Koh CL, Hooi PS, Wee KF, Khong JH, Chua BH, Chan YP, Lim ME, Lam SK (2002) Isolation of Nipah virus from Malaysian Island flying-foxes. Microbes Infect 4(2):145–151. https://doi.org/10.1016/S1286-4579(01)01522-2

6. Leroy EM, Kumulungui B, Pourrut X, Rouquet P, Hassanin A, Yaba P, Délicat A, Paweska JT, Gonzalez JP, Swanepoel R (2005) Fruit bats as reservoirs of Ebola virus. Nature 438:575–576. https://doi.org/10.1038/438575a

7. McFarlane R, Becker N, Field H (2011) Investigation of the climatic and environmental context of Hendra virus spillover events

1994–2010. PLoS ONE 6(12):e28374. https://doi.org/10.1371/journal.pone.0028374

8. Nikolay B, Salje H, Hossain MJ, Khan AKMD, Sazzad HMS, Rahman M, Daszak P, Ströher U, Pulliam JRC, Kilpatrick AM, Nichol ST, Klena JD (2019) Transmission of Nipah virus-14 years of investigations in Bangladesh. N Engl J Med 380(19):1804–1814. https://doi.org/10.1056/NEJMoa1805376

9. Tan CW, Wittwer K, Lim XF, Uehara A, Mani S, Wang LF, Anderson DE (2019) Serological evidence and experimental infection of cynomolgus macaques with *Pteropine orthoreovirus* reveal monkeys as potential hosts for transmission to humans. Emerg Microbes Infect 8(1):787–795. https://doi.org/10.1080/22221751.2019.1621668

10. Gard G, Compans RW (1970) Structure and cytopathic effects of Nelson Bay virus. J Virol 6(1):100–106

11. Hu T, Qiu W, He B, Zhang Y, Yu J, Liang X, Zhang W, Chen G, Zhang Y, Wang Y, Zheng Y, Feng Z, Hu Y, Zhou W, Tu C, Fan Q, Zhang F (2014) Characterization of a novel orthoreovirus isolated from fruit bat. China BMC Microbiol. 14:293–300. https://doi.org/10.1186/s12866-014-0293-4

12. Pritchard LI, Chua KB, Cummins D, Hyatt A, Crameri G, Eaton BT, Wang LF (2006) Pulau virus; a new member of the Nelson Bay *Orthoreovirus* species isolated from fruit bats in Malaysia. Arch Virol 151(2):229–239. https://doi.org/10.1007/s00705-005-0644-4

13. Takemae H, Basri C, Mayasari NLPI, Tarigan R, Shimoda H, Omatsu T, Supratikno Pramono D, Cahyadi DD, Kobayashi R, Iida K, Mizutani T, Maeda K, Agungpriyono S, Hondo E (2018) Isolation of *Pteropine orthoreovirus* from *Pteropus vampyrus* in Garut, Indonesia. Virus Genes 54(6):823–827. https://doi.org/10.1007/s11262-018-1603-y

14. Taniguchi S, Maeda K, Horimoto T, Masangkay JS, Puentespina R, Alvarez J, Eres E, Cosico E, Nagata N, Egawa K, Singh H, Fukuma A, Yoshikawa T, Tani H, Fukushi S, Tsuchiaka S, Omatsu T, Mizutani T, Une Y, Yoshikawa Y, Shimojima M, Saijo M, Kyuwa S (2017) First isolation and characterization of *Pteropine orthoreoviruses* in fruit bats in the Philippines. Arch Virol 162(6):1529–1539. https://doi.org/10.1007/s00705-017-3251-2

15. Chua KB, Voon K, Crameri G, Tan HS, Rosli J, McEachern JA, Suluraju S, Yu M, Wang LF (2008) Identification and characterization of a new orthoreovirus from patients with acute respiratory infections. PLoS ONE 3(11):e3803. https://doi.org/10.1371/journal.pone.0003803

16. Singh H, Shimojima M, Ngoc TC, Quoc Huy NV, Chuong TX, Le Van A, Saijo M, Yang M, Sugamata M (2015) Serological evidence of human infection with *Pteropine orthoreovirus* in Central Vietnam. J Med Virol 87(12):2145–2148. https://doi.org/10.1002/jmv.24274

17. Uehara A, Tan CW, Mani S, Chua KB, Leo YS, Anderson DE, Wang LF (2019) Serological evidence of human infection by bat orthoreovirus in Singapore. J Med Virol 91(4):707–710. https://doi.org/10.1002/jmv.25355

18. Voon K, Tan YF, Leong PP, Teng CL, Gunnasekaran R, Ujang K, Chua KB, Wang LF (2015) *Pteropine orthoreovirus* infection among out-patients with acute upper respiratory tract infection in Malaysia. J Med Virol 87(12):2149–2153. https://doi.org/10.1002/jmv.24304

19. Cheng P, Lau C, Lai A, Ho E, Leung O, Chan F, Wong A, Lim W (2009) A novel reovirus isolated from a patient with acute respiratory disease. J Clin Virol 45(1):79–80. https://doi.org/10.1016/j.jcv.2009.03.001

20. Yamanaka A, Iwakiri A, Yoshikawa T, Sakai K, Singh H, Himeji D, Kikuchi I, Ueda A, Yamamoto S, Miura M, Shioyama Y, Kawano K, Nagaishi T, Saito M, Minomo M, Iwamoto N, Hidaka Y, Sohma H, Kobayashi T, Kanai Y, Kawagishi T, Nagata N, Fukushi S, Mizutani T, Tani H, Yaniguchi S, Fukuma

A, Shimojima M, Kurane I, Kageyama T, Odagiri T, Saijo M, Morikawa S (2014) Imported case of acute respiratory tract infection associated with a member of species Nelson Bay orthoreovirus. PLoS ONE 9(3):e92777. https://doi.org/10.1371/journal.pone.0092777

21. Kawagishi T, Kanai Y, Tani H, Shimojima M, Saijo M, Matsuura Y, Kobayashi T (2016) Reverse genetics for fusogenic Bat-Borne orthoreovirus associated with acute respiratory tract infections in humans: role of outer capsid protein σC in viral replication and pathogenesis. PLoS Pathog 12(2):e1005455. https://doi.org/10.1371/journal.ppat.1005455

22. Egawa K, Shimojima M, Taniguchi S, Nagata N, Tani H, Yoshikawa T, Kurosu T, Watanabe S, Fukushi S, Saijo M (2017) Virulence, pathology, and pathogenesis of *Pteropine orthoreovirus* (PRV) in BALB/c mice: development of an animal infection model for PRV. PLoS Negl Trop Dis 11(12):e0006076. https://doi.org/10.1371/journal.pntd.0006076

23. Kanai Y, Kawagishi T, Okamoto M, Sakai Y, Matsuura Y, Kobayashi T (2018) Lethal murine infection model for human respiratory disease-associated *Pteropine orthoreovirus*. Virology 514:57–65. https://doi.org/10.1016/j.virol.2017.10.021

24. Middleton DJ, Morrissy CJ, Van Der Heide BM, Russell GM, Braun MA, Westbury HA, Halpin K, Daniels PW (2007) Experimental Nipah virus infection in pteropid bats (*Pteropus poliocephalus*). J Comp Pathol 136(4):266–272. https://doi.org/10.1016/j.jcpa.2007.03.002

25. Munster VJ, Adney DR, Van Doremalen N, Brown VR, Miazgowicz KL, Milne-Price S, Bushmaker T, Rosenke R, Scott D, Hawkinson A, De Wit E, Schountz T, Bowen RA (2016) Replication and shedding of MERS-CoV in Jamaican fruit bats (*Artibeus jamaicensis*). Sci Rep 6:21878. https://doi.org/10.1038/srep21878

26. Paweska JT, Storm N, Grobbelaar AA, Markotter W, Kemp A, Van Vuren PJ (2016) Experimental inoculation of Egyptian fruit bats (*Rousettus aegyptiacus*) with Ebola virus. Viruses 8(2):29. https://doi.org/10.3390/v8020029

27. Meylan E, Tschopp J (2006) Toll-like receptors and RNA helicases: two parallel ways to trigger antiviral responses. Mol Cell 22(5):561–569. https://doi.org/10.1016/j.molcel.2006.05.012

28. Li J, Zhang G, Cheng D, Ren H, Qian M, Du B (2015) Molecular characterization of RIG-I, STAT-1 and IFN-beta in the horseshoe bat. Gene 561(1):115–123. https://doi.org/10.1016/j.gene.2015.02.013

29. Sarkis S, Lise MC, Darcissac E, Dabo S, Falk M, Chaulet L, Neuveut C, Meurs EF, Lavergne A, Lacoste V (2018) Development of molecular and cellular tools to decipher the type I IFN pathway of the common vampire bat. Dev Comp Immunol 81:1–7. https://doi.org/10.1016/j.dci.2017.10.023

30. Tarigan R, Shimoda H, Doysabas KCC, Maeda K, Iida A, Hondo E (2020) Role of pattern recognition receptors and interferon-beta in protecting bat cell lines from encephalomyocarditis virus and Japanese encephalitis virus infection. Biochem Biophys Res Commun 527(1):1–7. https://doi.org/10.1016/j.bbrc.2020.04.060

31. Takadate Y, Kondoh T, Igarashi M, Maruyama J, Manzoor R, Ogawa H, Kajihara M, Furuyama W, Sato M, Miyamoto H, Yoshida R, Hill TE, Freiberg AN, Feldmann H, Marzi A, Takada A (2020) Niemann-pick C1 heterogeneity of bat cells controls Filovirus tropism. Cell Rep 30(2):308–319. https://doi.org/10.1016/j.celrep.2019.12.042

32. Maruyama J, Miyamoto H, Kajihara M, Ogawa H, Maeda K, Sakoda Y, Yoshida R, Takada A (2014) Characterization of the envelope glycoprotein of a novel Filovirus, Lloviu virus. J Virol 88(1):99–109. https://doi.org/10.1128/JVI.02265-13

33. Takadate Y, Manzoor R, Saito T, Kida Y, Maruyama J, Kondoh T, Miyamoto H, Ogawa H, Kajihara M, Igarashi M, Takada A (2020) Receptor-mediated host cell preference of a bat-derived Filovirus,

Lloviu virus. Microorganisms 8(10):1530–1542. https://doi.org/10.3390/microorganisms8101530

34. Maruyama J, Nao N, Miyamoto H, Maeda K, Ogawa H, Yoshida R, Igarashi M, Takada A (2016) Characterization of the glycoproteins of bat-derived influenza viruses. Virology 488:43–50. https://doi.org/10.1016/j.virol.2015.11.002

35. Katoh H, Kubota T, Ihara T, Maeda K, Takeda M, Kidokoro M (2016) Cross-neutralization between human and African bat mumps viruses. Emerg Infect Dis 22(4):703–706. https://doi.org/10.3201/eid2204.151116

36. Maeda K, Hondo E, Terakawa J, Kiso Y, Nakaichi N, Endoh D, Sakai K, Morikawa S, Mizutani T (2008) Isolation of novel adenovirus from fruit bat (*Pteropus dasymallus yayeyamae*). Emerg Infect Dis 14(2):347–349. https://doi.org/10.3201/eid1402.070932

37. Schmittgen TD, Livak KJ (2008) Analyzing real-time PCR data by the comparative C_T method. Nat Protoc 3:1101–1108. https://doi.org/10.1038/nprot.2008.73

38. Höbel S, Aigner A (2010) Polyethylenimine (PEI)/siRNA-mediated gene knockdown in vitro and in vivo. In: Min WP, Ichim T (eds) RNA interference: from biology to clinical application. Humana Press, New York, pp 283–297

39. Ciechonska M, Duncan R (2014) Reovirus FAST proteins: virus-encoded cellular fusogens. Trends Microbiol 22(12):715–724. https://doi.org/10.1016/j.tim.2014.08.00

40. Hemann EA, Gale M Jr., Savan R (2017) Interferon lambda genetics and biology in regulation of viral control. Front Immunol 8:1–12. https://doi.org/10.3389/fimmu.2017.01707

41. Liu WJ, Wang XJ, Clark DC, Lobigs M, Hall RA, Khromykh AA (2006) A single amino acid substitution in the West Nile virus nonstructural protein NS2A disables its ability to inhibit alpha/beta interferon induction and attenuates virus virulence in mice. J Virol 80(5):2396–2404. https://doi.org/10.1128/JVI.80.5.2396-2404.2006

42. Mok L, Wynne JW, Grimley S, Shiell B, Green D, Monaghan P, Pallister J, Bacic A, Michalski WP (2015) Mouse fibroblast L929 cells are less permissive to infection by Nelson Bay orthoreovirus compared to other mammalian cell lines. J Gen Virol 96(Pt 7):1787–1794. https://doi.org/10.1099/vir.0.000112

43. Irving A, Zhang Q, Kong PS, Luko K, Rozario P, Wen M, Zhu F, Zhou P, Ng JHJ, Sobota RM, Wang LF (2020) Directly regulate gene expression in bats in response to viral infection. Cell Rep 33:108345. https://doi.org/10.1016/j.celrep.2020.108345

44. Kato H, Takeuchi O, Sato S, Yoneyama M, Yamamoto M, Matsui K, Uematsu S, Jung A, Kawai T, Ishii KJ, Yamaguchi O, Otsu K, Tsujimura T, Koh CS, Sousa CRE, Matsuura Y, Fujita T, Akira S (2006) Differential roles of MDA5 and RIG-I helicases in the recognition of RNA viruses. Nature 441(7089):101–105. https://doi.org/10.1038/nature04734

45. Sherry B (2009) Rotavirus and reovirus modulation of the interferon response. J Interf Cytokine Res 29(9):559–567. https://doi.org/10.1089/jir.2009.0072

46. Banerjee A, Falzarano D, Rapin N, Lew J, Misra V (2019) Interferon regulatory factor 3-mediated signaling limits Middle-East respiratory syndrome (MERS) coronavirus propagation in cells from an insectivorous bat. Viruses 11(2):152. https://doi.org/10.3390/v11020152

47. Banerjee A, Rapin N, Bollinger T, Misra V (2017) Lack of inflammatory gene expression in bats: a unique role for a transcription repressor. Sci Rep 7(1):1–15

48. Ahn M, Anderson DE, Zhang Q, Tan CW, Lim BL, Luko K, Wen M, Chia WN, Mani S, Wang LC, Ng JHJN, Sobota RM, Dutertre CA, Ginhoux F, Shi ZL, Irving AT, Wang LF (2019) Dampened NLRP3-mediated inflammation in bats and implications for a special viral reservoir host. Nat Microbiol 4:789–799. https://doi.org/10.1038/s41564-019-0371-3

49. Farone AL, O'Brien PC, Cox DC (1993) Tumor necrosis factor-α induction by reovirus serotype 3. J Leukoc Biol 53(2):133–137. https://doi.org/10.1002/jlb.53.2.133

50. Farone AL, O'donnell SM, Brooks CS, Young KM, Pierce JM, Wetzel JD, Dermody TS, Farone MB (2006) Reovirus strain-dependent inflammatory cytokine responses and replication patterns in a human monocyte cell line. Viral Immunol 19(3):546–557. https://doi.org/10.1089/vim.2006.19.546

51. Jiang RD, Li B, Liu XL, Liu MQ, Chen J, Luo DS, Hu BJ, Zhang W, Li SY, Yang XL, Shi ZL (2020) Bat mammalian orthoreoviruses cause severe pneumonia in mice. Virology 551:84–92. https://doi.org/10.1016/j.virol.2020.05.014

52. Rivera CDLCR, Kanchwala M, Liang H, Kumar A, Wang LF, Xing C, Schoggins JW (2018) The IFN response in bats displays distinctive IFN-stimulated gene expression kinetics with atypical RNASEL induction. J Immunol 200(1):209–217. https://doi.org/10.4049/jimmunol.1701214

53. Kato H, Takeuchi O, Satoh EM, Hirai R, Kawai T, Matsushita K, Hiiragi A, Dermody TS, Fujita T, Akira S (2008) Length-dependent recognition of double-stranded ribonucleic acids by retinoic acid–inducible gene-I and melanoma differentiation–associated gene 5. J Exp Med 205(7):1601–1610. https://doi.org/10.1084/jem.20080091

54. Kuzmin IV, Schwarz TM, Ilinykh PA, Jordan I, Ksiazek TG, Sachidanandam R, Basler CF, Bukreyev A (2017) Innate immune response of bat and human cells to Filoviruses: commonalities and distinction. J Virol 91:e02471. https://doi.org/10.1128/JVI.02471-16

55. Mok L, Wynne JW, Tachedjian M, Shiell B, Ford K, Matthews DA, Bacic A, Michalski WP (2017) Proteomics informed by transcriptomics for characterising differential cellular susceptibility to Nelson Bay orthoreovirus infection. BMC Genom 18(1):615. https://doi.org/10.1186/s12864-017-3994-x

56. Irving AT, Rozario P, Kong PS, Luko K, Gorman JJ, Hastie ML, Chia WN, Mani S, Lee BPH, Smith GJD, Mendenhall IH, Larman HB, Elledge SJ, Wang LF (2020) Robust dengue virus infection in bat cells and limited innate immune response coupled with positive serology from bats in IndoMalaya and Australasia. Cell Mol Life Sci 77(8):1607–1622. https://doi.org/10.1007/s00018-019-03242-x

57. Zhou P, Cowled C, Wang LF, Baker ML (2013) Bat Mx1 and Oas1, but not Pkr are highly induced by bat interferon and viral infection. Dev Comp Immunol 40(3–4):240–247. https://doi.org/10.1016/j.dci.2013.03.006

58. Zhou P, Cowled C, Todd S, Crameri G, Virtue ER, Marsh GA, Klein R, Shi Z, Wang LF, Baker ML (2011) Type III IFNs in pteropid bats: differential expression patterns provide evidence for distinct roles in antiviral immunity. J Immunol 186(5):3138–3147. https://doi.org/10.4049/jimmunol.1003115

59. Banerjee A, Zhang X, Yip A, Schulz K, Irving AT, Bowdish D, Golding B, Wang LF, Mossman K (2020) Positive selection of a serine residue in bat IRF3 confers enhanced antiviral protection. iScience 23(3):100958. https://doi.org/10.1016/j.isci.2020.100958